Gerwig, G. J., Kamerling, J. P., & Vliegenthart, J. F. G. (1978) *Carbohydr. Res. 62*, 349-357.
Good, R. C. (1985) *Annu. Rev. Microbiol. 39*, 347-369.
Goren, M. B., & Brennan, P. J. (1979) in *Tuberculosis* (Youmans, G. P., Ed.) pp 69-193, Saunders, Philadelphia.
Gray, G. R. (1976) *Methods Carbohydr. Chem. 7*, 157-159.
Hakomori, S. (1964) *J. Biochem. (Tokyo) 55*, 205-208.
Hunter, S. W., Murphy, R. C., Clay, K., Goren, M. B., & Brennan, P. J. (1983) *J. Biol. Chem. 258*, 10481-10487.
Hunter, S. W., Jardine, I., Yanagihara, D. L., & Brennan, P. J. (1985) *Biochemistry 24*, 2798-2805.
Janssen, P. E., Kenne, L., Liedgren, H., Lindberg, B., & Lonngren, J. (1976) *Chem. Commun., Univ. Stockholm No. 8*, 1-75.
Jonsson, G. P., Hedin, A. B., Hakansson, P. L., Sundqvist, B. U. R., Save, B. G. S., Nielsen, P. F., Roepstorff, P., Johansson, K.-E., Kamensky, I., & Lindberg, M. S. L. (1986) *Anal. Chem. 58*, 1084-1087.
Kamisango, K., Saadat, S., Dell, A., & Ballou, C. E. (1985) *J. Biol. Chem. 260*, 4117-4121.
Kasai, R., Okihara, M., Asakawa, J., Mizutani, K., & Tanaka, O. (1979) *Tetrahedron 35*, 1427-1432.
Kim, K. S., Salton, M. R. J., & Barksdale, L. (1976) *J. Bacteriol. 125*, 739-743.
Lemieux, R. V., & Stevens, J. D. (1966) *Can. J. Chem. 44*, 249-262.
Lindberg, B. (1972) *Methods Enzymol. 28*, 178-195.
Marks, J., Jenkins, P. A., & Tsukamura, M. (1972) *Tubercle 53*, 210-214.
McNeil, M., Tsang, A. Y., & Brennan, P. J. (1987) *J. Biol. Chem. 262*, 2630-2635.
Minnikin, D. E. (1982) in *The Biology of the Mycobacteria* (Ratledge, C., & Stanford, J., Eds.) Vol. 2, pp 95-184, Academic, London.
Minnikin, D. E., Dobson, G., Sesardic, D., & Ridell, M. (1985) *J. Gen. Microbiol. 131*, 1369-1374.
Mort, A. J., & Bauer, W. D. (1982) *J. Biol. Chem. 257*, 1870-1875.
Park, J. T., & Johnson, M. J. (1949) *J. Biol. Chem. 181*, 149-151.
Prehm, P. (1980) *Carbohydr. Res. 78*, 372-374.
Saadat, S., & Ballou, C. E. (1983) *J. Biol. Chem. 258*, 1813-1818.
Schaefer, W. B. (1965) *Am. Rev. Respir. Dis. 92 (Suppl.)*, 85-93.
Schaefer, W. B., Wolinsky, E., Jenkins, P. A., & Marks, J. (1973) *Am. Rev. Respir. Dis. 108*, 1320-1326.
Schleifer, K. H., & Kandler, O. (1972) *Bacteriol. Rev. 36*, 407-477.
Skerman, V. B. D., McGowen, V., & Sneath, P. H. A. (1980) *Int. J. Syst. Bacteriol. 30*, 225-240.
Sundqvist, B., Kamensky, I., Hakansson, J., Kjellberg, J., Salehpour, M., Widdiyasekera, S., Fohlman, J., Peterson, P. A., & Roepstorff, P. (1984) *Biomed. Mass Spectrom. 11*, 242-257.
Takayama, K., Schones, H. K., Armstrong, E. L., & Boyle, R. W. (1975) *J. Lipid Res. 16*, 308-317.
Vilkas, E., Adam, A., & Senn, M. (1968) *Chem. Phys. Lipids 2*, 11-16.
Wayne, L. G. (1986) *CRC Crit. Rev. Microbiol. 12*, 185-222.
Wolinsky, F. (1979) *Am. Rev. Respir. Dis. 119*, 107-159.
Yanagihara, D. L., Barr, V. L., Knisley, C. V., Tsang, A. Y., McClatchy, J. K., & Brennan, P. J. (1985) *J. Clin. Microbiol. 21*, 569-574.

Volume Changes during Enzyme Reactions: Indications of Enzyme Pulsation during Fumarase Catalysis†

Peter Butz, Karl O. Greulich, and Horst Ludwig*
Institut für Physikalische Chemie, Universität Heidelberg, Im Neuenheimer Feld 253, D-6900 Heidelberg, FRG
Received May 1, 1987; Revised Manuscript Received September 17, 1987

ABSTRACT: Overall activation volumes for multistep reactions are not usually pressure independent. The present investigation gives a quantitative description of this effect under Theory. Simple relations are obtained which can easily be applied to experimental data and which allow more insight into the dynamics of enzyme reactions. This is demonstrated under Experimental Application for the conversion of fumarate to L-malate catalyzed by the enzyme fumarase. The volume profile of this reaction indicates a pulsation of the enzyme molecule during catalysis. The appendix discusses the question whether Eyring's transition-state theory is an appropriate basis for investigations of this kind.

Although pressure is a thermodynamic parameter as important as temperature, it has long been disregarded and has only lately gained importance in biology and biochemistry. High-pressure experiments have revealed the role of membranes in anesthetics (Lodge, 1985) and the action of ethanol (Alkana et al., 1985). Pressure affects the photocycle of purple membranes (Marque & Eisenstein, 1984) probably because the charge transfer through the membrane is affected (Canfield & Macey, 1984). Hydrostatic pressure has been used to kill bacteria, spores, yeasts, and molds in order to sterilize sensitive pharmaceutical products (Butz & Ludwig, 1986; Mentrup et al., 1988). When applied to fertilized eggs, high-pressure produces triploid cells (Vasetskii et al., 1985), probably by inhibiting microtubule assembly and spindle formation, and may become an interesting tool for the study of genetic diseases such as trisomies. Pressure-inactivated lymphocytes have been used in multiple sclerosis research (Cohen, 1985). Another promising application seems to be the use of high pressure for the isolation of certain membrane

† This research was partly supported by the Bundesministerium für Forschung und Technologie.

0006-2960/88/0427-1556$01.50/0

proteins (Deckmann et al., 1985). On a more molecular basis, pressure has been used to study the refolding and dissociation of enzymes (Krebs et al., 1985; Verjovski-Almeida et al., 1986), the association of melittin (Thompson & Lakowicz, 1984), and the self-assembly of actin (Swezey & Somero, 1985). Many other examples can be found in the reviews of Heremans (1978) and of Weber (1983).

Most of the experiments summarized above are still waiting to be interpreted. There seems to be a need for a more detailed understanding of the underlying processes. Very important parameters in explaining pressure effects are the reaction volume of the process under study and the activation volumes of the single elementary steps. Thus, high-pressure studies may provide supplemental information on protein dynamics (Kauzmann, 1987) recently studied by solution compressibility and X-ray crystallography (Gekko & Hasegawa, 1986; Frauenfelder et al., 1987).

In an attempt to understand the role of single activation volumes and reaction volumes in relation to the influence of pressure on reaction rates, we have investigated a few sugar-converting enzymes (Ludwig & Greulich, 1978) and now present a general study on pressure effects in enzymatic reactions. The theoretical considerations are exemplified by the enzyme fumarase, which catalyzes the conversion of fumarate to L-malate reversibly.

Theory

Introduction. According to the transition-state theory, the pressure dependence of a rate constant is given by the relation

$$\left(\frac{\mathrm{d}\ln k}{\mathrm{d}p}\right)_T = -\frac{\Delta V^{\ddagger}}{RT} \tag{1}$$

where k is the rate constant at pressure p and $\Delta V^{\ddagger}$ is the activation volume. If $\Delta V^{\ddagger}$ does not depend on p, eq 1 can be integrated to give

$$k/k_0 = e^{-\Delta V^{\ddagger} p/RT} \tag{1a}$$

The rate constant k_0 at zero pressure has practically the same value as the constant at normal pressure. According to eq 1a, a plot of ln (k/k_0) versus pressure is a straight line through the origin. For multistep reactions, pressure-dependent overall activation volumes are often observed, leading to deviations from linearity. One usually assumes that curvature is caused by compressibility effects (Le Noble, 1967; Eckert, 1972). In this work curvature is explained in terms of pressure-dependent single-step reaction rate constants. Methods for determining the corresponding single-step activation volumes are given.

Activation Volumes in Enzymatic Reactions. Enzyme reactions can often be described by the Michaelis–Menten mechanism:

$$\mathrm{E} + \mathrm{S} \underset{k_{-1}}{\overset{k_1}{\rightleftharpoons}} \mathrm{ES} \xrightarrow{k_2} \mathrm{E} + \mathrm{P} \tag{2}$$

The reaction rate is given by

$$v([\mathrm{S}]) = \frac{V[\mathrm{S}]}{K_\mathrm{m} + [\mathrm{S}]} \tag{3}$$

where $V = k_2[\mathrm{E}]_0$ (maximum velocity), $[\mathrm{E}]_0$ = total enzyme concentration, [S] = substrate concentration, P = product, and $K_\mathrm{m} = (k_{-1} + k_2)/k_1$ (Michaelis constant).

For many enzymatic reactions, e.g., the fumarase reaction, the Michaelis–Menten scheme has to be extended:

$$\mathrm{E} + \mathrm{F} \underset{k_{-1}}{\overset{k_1}{\rightleftharpoons}} \mathrm{EF} \xrightarrow{k_2} \mathrm{EM} \xrightarrow{k_3} \mathrm{E} + \mathrm{M} \tag{4}$$

where E is the enzyme and F and M are the substrates fumarate and L-malate. In this case eq 3 still holds, but V and K_m have other meanings:

$$V = \frac{k_3 k_2}{k_3 + k_2}[\mathrm{E}]_0 = k^{\mathrm{c}}[\mathrm{E}]_0 \tag{5}$$

$$K_\mathrm{m} = \frac{(k_{-1} + k_2)k_3}{k_1(k_2 + k_3)} \tag{6}$$

According to eq 1, each of the single-step reaction rate constants (k_i in eq 5 and 6) is dependent on pressure, but it is not possible to measure their corresponding activation volumes independently. In practice, one can determine two formal activation volumes by considering the pressure dependence of V, representing substrate saturation conditions, and of V/K_m, the rate constant at low substrate concentrations: $\Delta V^{\ddagger}_{\mathrm{c}}$ is the activation volume related to k^{c}, the rate constant at substrate saturation; $\Delta V^{\ddagger}_{\mathrm{o}}$ is the activation volume related to k^{o}, the rate constant at low substrate concentration ($k^{\mathrm{o}} = k^{\mathrm{c}}/K_\mathrm{m}$).

It has been shown (Ludwig & Greulich, 1978; Laidler, 1973) that the pressure dependence of k^{o} is obtained from eq 1 with the activation volume:

$$\Delta V^{\ddagger}_{\mathrm{o}} = \Delta V^{\ddagger}_1 + \frac{\Delta V^{\ddagger}_2 - \Delta V^{\ddagger}_{-1}}{1 + k_2/k_{-1}} \tag{7}$$

where $\Delta V^{\ddagger}_1$, $\Delta V^{\ddagger}_2$, and $\Delta V^{\ddagger}_{-1}$ are the activation volumes associated with k_1, k_2, and k_{-1}. A similar formula can be obtained for $\Delta V^{\ddagger}_{\mathrm{c}}$ by replacing the indices 1 and −1 by 3 in eq 7. Laidler (1973) limited the interpretation of eq 7 to the extreme cases $k_{-1} \ll k_2$ and $k_{-1} \gg k_2$, which gave pressure-independent values of $\Delta V^{\ddagger}_{\mathrm{o}}$. Other cases have not been discussed, and thus, some information is missing. To a small extent the pressure dependence of $\Delta V^{\ddagger}_{\mathrm{o}}$ may be caused by compressibility effects in $\Delta V^{\ddagger}_1$, $\Delta V^{\ddagger}_{-1}$, and $\Delta V^{\ddagger}_2$, but usually these are of the order of less than a few percent per kilobar; these effects are very small compared to those to be measured, the main part of which should be ascribed to the pressure dependence of the k_i values.

Introducing the pressure dependence of k_i according to eq 1 into eq 7, one obtains

$$\Delta V^{\ddagger}_{\mathrm{o}} = \Delta V^{\ddagger}_1 + \frac{\Delta V^{\ddagger}_2 - \Delta V^{\ddagger}_{-1}}{1 + \dfrac{k_{2,0}}{k_{-1,0}} \exp\left[-\dfrac{(\Delta V^{\ddagger}_2 - \Delta V^{\ddagger}_{-1})p}{RT}\right]} \tag{8}$$

where $k_{2,0}$ and $k_{-1,0}$ are the constants at normal pressure.

By substituting this expression for $\Delta V^{\ddagger}_{\mathrm{o}}$ in eq 1 and then integrating, the pressure dependence of k^{o} is obtained using the following abbreviations:

$$U = \Delta V^{\ddagger}_2 - \Delta V^{\ddagger}_{-1} \qquad a = k_{2,0}/k_{-1,0}$$

$$\ln \frac{k^{\mathrm{o}}}{k^{\mathrm{o}}_0} = -\frac{\Delta V^{\ddagger}_1}{RT}p - \ln \frac{\exp(Up/RT) + a}{1 + a} \tag{9}$$

Equation 9 and the corresponding equation for k^{c}, obtained by replacing the indices 1 and −1 by 3, are the fundamental equations bringing the measured effects in relation to single-step activation volumes and to ratios of single-step reaction rates. Plots of ln (k/k_0), k being k^{o} or k^{c}, against pressure yield hyperbolic curves through the origin. Because the second derivative of eq 9 is negative, the curves are always convex. Figure 1 shows the graphs for three cases, as they occur in the measurements under Experimental Application. Depending on the pressure range, negatively curved lines or straight lines with positive or negative slopes are obtained. Note that the abscissa in Figure 1 also covers the (physically

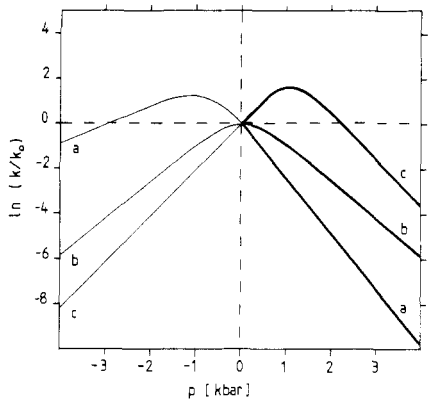

FIGURE 1: Graphs according to eq 9 including the negative pressure range. The curves are computed with the following parameters: (a) $\Delta V^{\ddagger}_1 = -20$, $U = 80$, and $a = 0.1$; (b) $\Delta V^{\ddagger}_1 = -40$, $U = 80$, and $a = 1.0$; (c) $\Delta V^{\ddagger}_1 = -50$, $U = 100$, and $a = 100$. Volumes in units of cubic centimeters per mole.

meaningless) negative pressure range.

Determination of Single-Step Activation Volumes. Having measured the pressure dependence of k^o and k^c for both directions of the reaction, one can determine the single-step activation volumes with the aid of eq 9. Two methods to evaluate the parameters $\Delta V^{\ddagger}$, U, and a in this equation are described later in this section.

First, it should be shown how k^o and k^c themselves are determined. Because the rate constants k^o and k^c are related to the enzyme kinetic constants V and K_m, as described under Activation Volumes in Enzymatic Reactions, one has to measure the pressure dependence of these kinetic constants. This can be achieved by measurement of initial velocities as a function of pressure and substrate concentration and subsequent application of the Lineweaver–Burk method to the data.

In our case a method of Greulich and Ludwig (1976) was applied, for which the absolute reaction rates are not required. Only the ratios v_p/v_0 are needed, and these can be derived from eq 3:

$$\frac{v_p}{v_0} = \frac{V_p}{V_0}\frac{K_m + [S]}{K_p + [S]} \tag{10}$$

where the indices p and 0 indicate elevated and normal pressure.

By defining the new variable Y as

$$Y = (v_p/v_0)/(K_m + [S])$$

and rearranging eq 10, one obtains

$$[S]Y = V_p/V_0 - K_pY \tag{11}$$

The slope and ordinate of a plot according to eq 11 yield K_p and V_p/V_0, from which k^o and k^c can be determined. This has to be done for all pressures applied.

The values of k^c and k^o at different pressures are the basis for the evaluation of the parameters $\Delta V^{\ddagger}$, U, and a in eq 9. This can be done by a graphical method or by nonlinear regression with the aid of an appropriate computer program.

For the graphical method, eq 9 is approximated by tangents at high and at low pressures. The asymptotic form of eq 9 for small pressure is given by

$$\left(\ln\frac{k^o}{k^o_0}\right)_{p\to 0} = -\frac{\Delta V^{\ddagger}_1 + U/(1+a)}{RT}p \tag{9a}$$

For high pressures, depending on whether $U < 0$ or $U > 0$, eq 9 reduces to

$$\left(\ln\frac{k^o}{k^o_0}\right)_{U>0,p\to\infty} = -\frac{\Delta V^{\ddagger}_1 + U}{RT}p + \ln(1+a) \tag{9b}$$

and

$$\left(\ln\frac{k^o}{k^o_0}\right)_{U<0,p\to\infty} = -\frac{\Delta V^{\ddagger}_1}{RT}p + \ln\left(1+\frac{1}{a}\right) \tag{9c}$$

It is not possible, however, to deduce from a given experimental curve whether U is negative or positive. Equations 9a–9c yield linear semilogarithmic plots of k^o/k^o_0 versus pressure, which give the following information:

	slope($-RT$)	ordinate intercept
(a) low pressure	$\Delta V^{\ddagger}_1 + U/(1+a)$	0
(b) high pressure, $U > 0$	$\Delta V^{\ddagger}_1 + U$	$\ln(1+a)$
(c) high pressure, $U < 0$	$\Delta V^{\ddagger}_1$	$\ln(1+1/a)$

Due to the uncertainty about the sign of U, there are always two sets of solutions. The solution with $U < 0$ can be evaluated from eq 9a combined with eq 9c. A combination of eq 9a with eq 9b yields the alternative solution with $U > 0$. Both sets are coupled by the relations

$$\Delta V^{\ddagger}_1{}' = \Delta V^{\ddagger}_1 + U \qquad U' = -U \qquad a' = 1/a$$

To decide which of the two sets is the right one, additional information is necessary, e.g., an estimate of a.

In this context it becomes clear that satisfactory results can only be obtained by application of short pressure intervals for measurements in the lower pressure region and that it is often difficult to draw the low-pressure tangent correctly (see Figure 1). These tangents can represent a considerable source of error in the evaluation of activation volumes. It therefore seems reasonable to use the graphically determined values as first estimates for a weighted computer analysis by nonlinear regression.

The volume profile of the reaction is established by combining the single-step activation volumes obtained, or combinations of them (e.g., $\Delta V^{\ddagger}_1 + \Delta V^{\ddagger}_2 - \Delta V^{\ddagger}_{-1}$), in such a manner that no inconsistency occurs. If more than one possible solution is found to describe the total reaction pathway from educts to products, knowledge of the reaction volume can be helpful since it represents the sum of the single-step activation volumes. The reaction volume can be determined from the pressure dependence of the equilibrium constant and by direct density measurement.

Experimental Application

Introduction. Fumarase or fumarate hydratase (EC 4.2.1.2), an essential enzyme of the citric acid cycle, catalyzes the reversible addition of water to fumarate, yielding L-malate. The enzyme has a M_r of 194 000 and is composed of four identical subunits. A comprehensive review has been given by Hill and Teipel (1971). The high-pressure enzyme kinetic data given by Andersen and Broe (1972) were inadequate for a treatment as shown under Theory. The aim of the present work was to show the practical applicability of our theoretical considerations.

Materials and Methods. (a) Basic Requirements. In high-pressure enzyme kinetics, some basic requirements have to be met to ensure the reliability and usability of the measured data. First, kinetic data should not be falsified by denaturation effects; the concentration of intact enzyme molecules must remain constant during the measurement. Second, it has to be taken into account that the basic equations under Theory are only valid for pressure-independent concentration units;

Table I: High-Pressure (hp) and Low-Pressure (lp) Extremes of $\Delta V^{\ddagger}_{o}$ and $\Delta V^{\ddagger}_{c}$ and Ordinate Intercepts of High-Pressure Tangents on Graphs According to eq 9 for Both Substrates (F and M)[a]

	$\Delta V^{\ddagger}_{o;F}$		$\Delta V^{\ddagger}_{o;M}$		$\Delta V^{\ddagger}_{c;F}$		$\Delta V^{\ddagger}_{c;M}$		ordinate intercepts for			
NaCl (mol/kg)	hp	lp	hp	lp	hp	lp	hp	lp	k^{o}_{F}	k^{o}_{M}	k^{c}_{F}	k^{c}_{M}
0.0	16.2	−21.1	27.7	27.7	24.9	4.9	27.7	27.7	1.04	0.0	0.31	0.0
0.1	19.6	−14.8	30.5	30.5	25.8	7.4	30.5	30.5	0.80	0.0	0.28	0.0
0.2	22.0	−14.8	30.6	30.6	29.2	20.8	30.6	30.6	0.75	0.0	0.12	0.0
0.3	23.5	−10.8	31.5	31.5	31.0	31.0	31.5	31.5	0.56	0.0	0.02	0.0

[a] Volumes in units of cubic centimeters per mole.

therefore, if spectroscopic velocity measurements are carried out, a suitable calibration is required. In this work, concentrations are given in molality (moles of solute per kilogram of solvent).

Further problems can arise from the high-pressure behavior of the solvent, because the pH of several buffers shows pressure dependence, as is the case with the phosphate buffers used in this work. However, it could be demonstrated (Butz, 1982) that this effect is negligible since the pH optimum of the reaction is shifted in the same fashion. The denaturation effects mentioned above were investigated by Butz (1986), who showed that no significant denaturation occurs under the experimental conditions applied in this work. A procedure to separate denaturation effects mathematically was described by Greulich and Ludwig (1976).

(*b*) *Experimental Procedures.* The spectroscopic measurements under pressure were performed in a high-pressure optical cell (4 kbar max), equipped with two sapphire windows of 10-mm optical width, manufactured by Dunze Hochdrucktechnik. The thermostated cell was inserted into a Pye Unicam SP-1800 recording spectrophotometer. Pressure was generated by an air-driven hydraulic pump of the type SC-10600-40.

The enzyme was purchased from Boehringer Mannheim, the substrates were disodium fumarate from Roth and disodium L-malate from Serva. The initial velocity measurements were carried out in 0.067 M phosphate buffers; the pH was 6.7 when fumarate was the substrate and 7.4 with L-malate. Salt effects were measured with sodium chloride (analytical grade) from Merck, taking into account the pH shift due to salt addition.

Experimental Results. Figure 2 shows the pressure dependence of the initial velocities at different substrate concentrations for both directions of the reaction. With malate as substrate (Figure 2b) exponential curves are found, while with fumarate (Figure 2a) there are deviations from the exponential form up to 1000 bar. Similar results were obtained in additional experimental series with sodium chloride added in three different concentrations.

From the initial velocities the enzyme kinetic constants are determined by application of the method described under Determination of Single-Step Activation Volumes; thus k^{c} and k^{o} can be determined. The pressure dependence of k^{c} and k^{o} is given in Figure 3, where ln (k/k_0) is plotted against pressure in accordance with eq 9 for three concentrations of added sodium chloride and without salt addition. With malate as substrate (Figure 3c) straight lines are obtained; the fumarate curves (Figure 3a,b) show the hyperbolic form described in the theoretical part of this work. From the slopes of these curves $\Delta V^{\ddagger}_{c}$ and $\Delta V^{\ddagger}_{o}$ can be determined; the resulting values are listed in Table I. Table II gives the meanings of these formal activation volumes and of the ordinate intercepts of plots according to eq 9. The volume profile of the reaction (Figure 4) was established by combining $\Delta V^{\ddagger}_{o}$ and $\Delta V^{\ddagger}_{c}$ of the forward and the reverse reaction (Table I and eq 9a–9c). A volume profile with no inconsistency was found with the parameters given in Table III. A second possible combination of volumes could be excluded after comparing the values for ratios of rate constants with those found in literature (Alberty & Pierce, 1957).

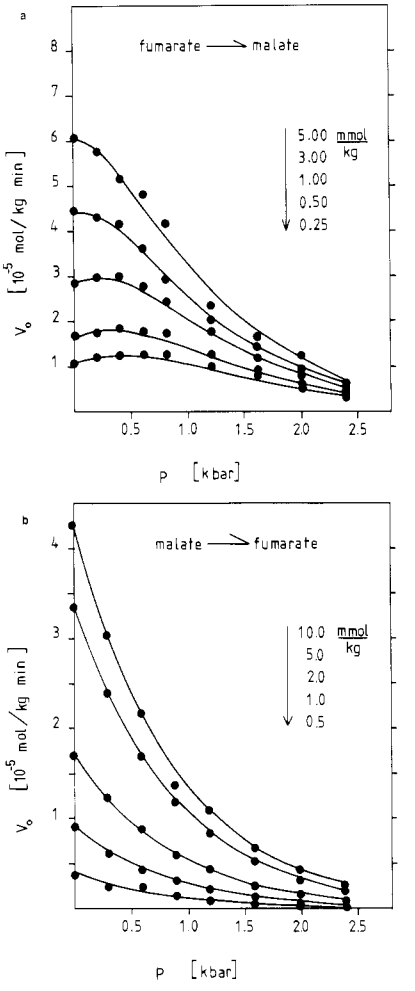

FIGURE 2: Pressure dependence of the initial velocities for the forward (a) and the reverse (b) reaction. The solid lines are computed from the results listed in Table I.

Table II: Meanings of the Formal Activation Volumes $\Delta V^{\ddagger}_{o}$ and $\Delta V^{\ddagger}_{c}$ and of the Ordinate Intercepts of Plots According to eq 9[a]

		$U > 0$	$U < 0$
$\Delta V^{\ddagger}_{o;F}$	hp	$\Delta V^{\ddagger}_{1} + \Delta V^{\ddagger}_{2} - \Delta V^{\ddagger}_{-1}$	$\Delta V^{\ddagger}_{1}$
	lp	$\Delta V^{\ddagger}_{1} + (\Delta V^{\ddagger}_{2} - \Delta V^{\ddagger}_{-1})/(1 + k_2/k_{-1})^{b}$	
$\Delta V^{\ddagger}_{o;M}$	hp	$\Delta V^{\ddagger}_{-3} + \Delta V^{\ddagger}_{-2} - \Delta V^{\ddagger}_{3}$	$\Delta V^{\ddagger}_{-3}$
	lp	$\Delta V^{\ddagger}_{-3} + (\Delta V^{\ddagger}_{-2} - \Delta V^{\ddagger}_{3})/(1 + k_{-2}/k_3)^{b}$	
$\Delta V^{\ddagger}_{c;F}$	hp	$\Delta V^{\ddagger}_{2}$	$\Delta V^{\ddagger}_{3}$
	lp	$\Delta V^{\ddagger}_{3} + (\Delta V^{\ddagger}_{2} - \Delta V^{\ddagger}_{3})/(1 + k_2/k_3)^{b}$	
$\Delta V^{\ddagger}_{c;M}$	hp	$\Delta V^{\ddagger}_{-2}$	$\Delta V^{\ddagger}_{-1}$
	lp	$\Delta V^{\ddagger}_{-1} + (\Delta V^{\ddagger}_{-2} - \Delta V^{\ddagger}_{-1})/(1 + k_{-2}/k_{-1})^{b}$	
ordinate intercepts	k^{o}_{F}	ln $(1 + k_2/k_{-1})$	ln $(1 + k_{-1}/k_2)$
	k^{o}_{M}	ln $(1 + k_{-2}/k_3)$	ln $(1 + k_3/k_{-2})$
	k^{c}_{F}	ln $(1 + k_2/k_3)$	ln $(1 + k_3/k_2)$
	k^{c}_{M}	ln $(1 + k_{-2}/k_{-1})$	ln $(1 + k_{-1}/k_{-2})$

[a] For symbols see Table I. [b] Valid for $U > 0$ and $U < 0$.

Table III: Single-Step Activation Volumes and Ratios of Rate Constants[a]

NaCl (mol/kg)	$\Delta V^{\ddagger}_1$	$\Delta V^{\ddagger}_{-1}$	$\Delta V^{\ddagger}_2$	$\Delta V^{\ddagger}_{-2}$	$\Delta V^{\ddagger}_3$	$\Delta V^{\ddagger}_{-3}$	k_2/k_{-1}	k_{-2}/k_3	k_2/k_3	k_{-2}/k_{-1}
0.0	−41.30	−32.60	24.90	27.70	−50.10	−50.10	1.82	small	0.363	small
0.1	−42.95	−36.75	25.75	30.50	−49.25	−49.25	1.23	small	0.323	small
0.2	−48.00	−40.75	29.25	30.55	−45.75	−45.75	1.11	small	0.127	small
0.3	−54.00	−46.55	30.95	31.55	−44.05	−44.05	0.75	small	0.020	small

[a] Volumes in units of cubic centimeters per mole. Volumes are given with four figures to make the calculations clearer. The values of the single volumes are to be rounded to integer numbers.

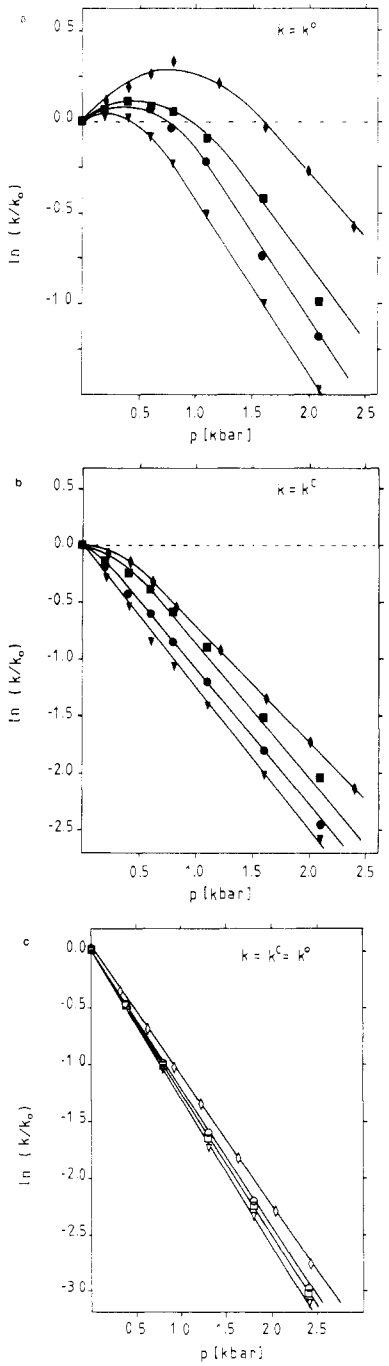

FIGURE 3: Pressure dependence of k^o and k^c with fumarate as substrate (a and b) and with L-malate (c) for four different salt concentrations: (♦) 0.0, (■) 0.1, (●) 0.2, and (▼) 0.3 mol/kg NaCl. The solid lines are computed from the results listed in Table I.

Discussion. On the basis of the theoretical considerations given under Theory of this work, the volume changes for each step of the fumarase reaction and for the overall reaction could be determined. The activation and reaction volumes may be caused by the volume changes of the substrates and the enzyme or by varying interactions with the solvent during the course

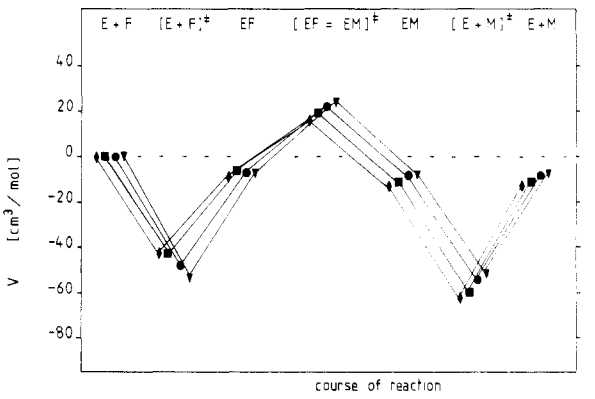

FIGURE 4: Volume profile of the enzyme-catalyzed reaction fumarate → L-malate for four different salt concentrations: (♦) 0.0, (■) 0.1, (●) 0.2, and (▼) 0.3 mol/kg NaCl. E, enzyme; F, fumarate; M, L-malate; EF and EM, enzyme–substrate complexes; [ ]‡, activated complex.

of the reaction. The solvent effects may be detected by addition of salt, as has been done in this work. If the concentration of charges or polar groups alters during a reaction, electrostrictive volume changes can occur due to changed solvent density around electrostatically active groups. By the addition of salt these effects are reduced due to shielding of these groups.

Another kind of volume change by solute–solvent interactions originates in conformational changes of a protein which are accompanied by the transfer of charged or hydrophobic groups from the more hydrophobic interior of the globular protein to the aqueous solution or vice versa. The transfer of 1-propanol from tetrachloromethane, a model for hydrophobic environment, to water, for example, causes a decrease in the volume of 6.4 cm³/mol (Duboc, 1969). If the solution contains a salt, e.g., NaCl, the water structure is influenced and the magnitude of the volume effect differs. Consequently, changed exposure of enzyme groups to the solvent is detected by testing the influence of NaCl on the activation volumes.

(*a*) $\Delta V^{\ddagger}_c$. The activation volume at high substrate concentration is pressure dependent for fumarate as substrate but not for malate (Figure 3). At high pressures, for both substrates, the activation volumes approach each other at a value around 25 cm³/mol (Table I).

When salt is added, all values for $\Delta V^{\ddagger}_c$ increase to approximately 31 cm³/mol. Low and Somero (1975) stated that salts which increase $\Delta V^{\ddagger}_c$ invariably decrease the rate of reaction and vice versa. This is confirmed in the case of fumarase, which is inhibited by sodium chloride.

With fumarate as substrate, the low-pressure activation volume (5 cm³/mol) approximates the high-pressure value (31 cm³/mol) more and more when salt is added. This is due to a major change in the parameter a in eq 9 (from 0.36 to 0.02), while $\Delta V^{\ddagger}_3$ is only slightly increased (−50.1 to −44.05 cm³/mol) and U remains constant at 75 cm³/mol. By virtue of these changes, the graph according to eq 9 is turned slightly clockwise and shifted to the upper left; thus the curvature disappears from the measurable part of Figure 4. In this case

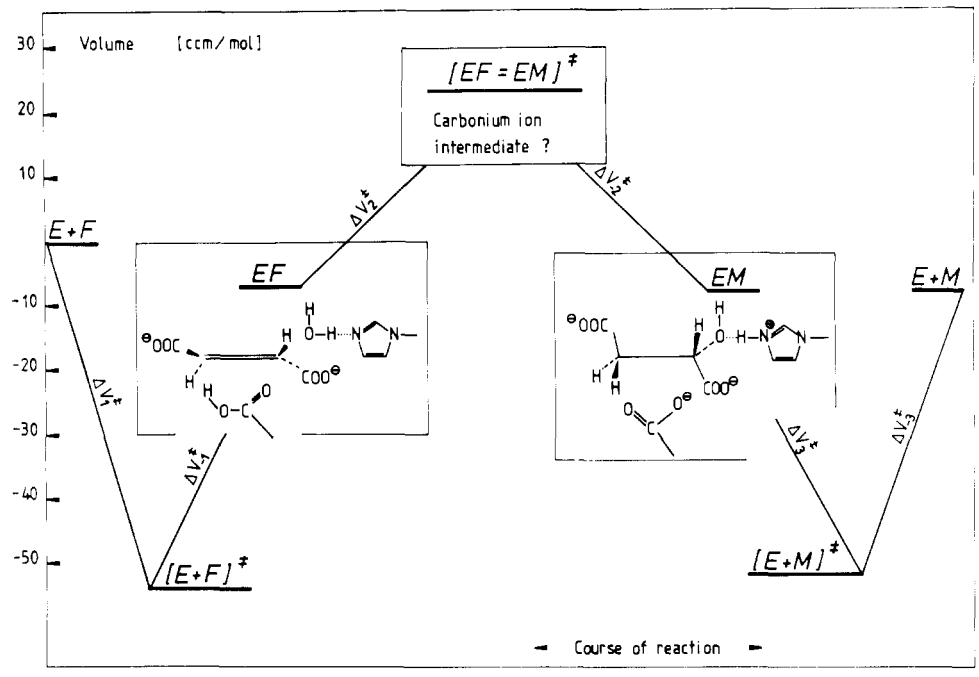

FIGURE 5: Volume profile of the reaction at high salt concentration (0.3 mol/kg) including a chemical mechanism [from Cleland (1977)] of the active site.

the parameter a is k_2/k_3 and U represents $\Delta V^{\ddagger}_2 - \Delta V^{\ddagger}_3$. The pressure dependence of k_2 and k_3 is obviously not much influenced by added salt. But there is a significant change in the ratio of k_2 and k_3 at normal pressure. This salt-induced rate change cannot be sufficiently explained by the salt-induced volume changes; the major source of rate changes is the salt influence on $\Delta U^{\ddagger}$ and $\Delta S^{\ddagger}$, as has been comprehensively discussed by Greaney and Somero (1979).

(*b*) $\Delta V^{\ddagger}_o$. The activation volume at low substrate concentration with fumarate as substrate shows an even stronger pressure dependence than $\Delta V^{\ddagger}_c$ (40 cm^3/mol difference in the measured pressure range instead of 20 cm^3/mol). For the reverse reaction $\Delta V^{\ddagger}_o$ is the same as $\Delta V^{\ddagger}_c$.

When salt is added, all activation volumes increase as was found for $\Delta V^{\ddagger}_c$. The $\Delta V^{\ddagger}_o$ value for the forward reaction is altered by salt addition in a way different than $\Delta V^{\ddagger}_c$; the parameter a remains nearly constant (1.82 to 0.75), but there is a major change in $U = \Delta V^{\ddagger}_2 - \Delta V^{\ddagger}_{-1}$ from 57.5 to 77.5 cm^3/mol. For the reverse reaction, $\Delta V^{\ddagger}_o$ rises from 27.7 to 31.5 cm^3/mol, as is the case for $\Delta V^{\ddagger}_c$.

One can see from this that increasing substrate concentration, salt addition, and pressure elevation take effect in the same direction: $\Delta V^{\ddagger}_c$ and $\Delta V^{\ddagger}_o$ tend to reach a value of about 31 cm^3/mol while the upper limit of U seems to be around 75 cm^3/mol, which implies that $\Delta V^{\ddagger}_{-1} = \Delta V^{\ddagger}_3$, since $\Delta V^{\ddagger}_2 - \Delta V^{\ddagger}_3 = \Delta V^{\ddagger}_2 - \Delta V^{\ddagger}_{-1} = 75$ cm^3/mol. From Table III one can see that this is the case for the highest salt concentration applied, where $\Delta V^{\ddagger}_{-1} = -46.55$ cm^3/mol and $\Delta V^{\ddagger}_3 = -44.05$ cm^3/mol. Additionally, a striking symmetry is found in the corresponding volume profile at high salt concentration with the symmetry axis in $(EF = EM)^{\ddagger}$ (i.e., $\Delta V^{\ddagger}_{-1} \approx \Delta V^{\ddagger}_3$, $\Delta V^{\ddagger}_2 \approx \Delta V^{\ddagger}_{-2}$, and $\Delta V^{\ddagger}_I \approx \Delta V^{\ddagger}_{-3} + \Delta V^{R}$), as if under these conditions the active site of the enzyme did not distinguish between the two substrates. Deviations from this symmetry as seen at lower salt concentrations must, in turn, be explained by solvent effects as described above.

Generally the measurements with fumarate as substrate yield more information due to the more complicated pressure dependence which can be explained by a change of the rate-limiting step induced by relatively small changes of pressure.

Table IV: Reaction Volume[a] by Two Different Methods

NaCl (mol/kg)	ΔV^{R}_{exp}[b]	$\Delta V^{R} = \sum_i \Delta V^{\ddagger}_i$[c]
0.0	−11.2	−11.50
0.1	−9.2	−10.95
0.2	−8.0	−8.55
0.3	−6.8	−8.00

[a] Volumes in units of cubic centimeters per mole. [b] From measurements of the pressure dependence of the equilibrium constant. [c] From Figure 4 or Table III.

Similar findings were reported for the temperature dependence of this reaction (Massey, 1953).

(*c*) ΔV^{R}. The overall volume difference, the reaction volume, can be taken from Figure 4 for varying concentrations of added salt. These values agree excellently with those we determined directly via the pressure dependence of the equilibrium constant (see Table IV).

The reaction volume is given by the difference of the partial molar volumes of malate on the one hand and fumarate and water on the other, the latter being, nearly independent of salt addition, 18 cm^3/mol in the measured range of concentrations. Thus the difference of the partial molar volumes of the two substrates could be calculated:

$$V_{malate} - V_{fumarate} = \Delta V^{R} + V_{water}$$

With $V_{water} = 18$ cm^3 and the measured ΔV^{R} from Table IV, the differences are 6.8, 8.84, 9.97, and 11.15 cm^3/mol for 0.0, 0.1, 0.2, and 0.3 mol/kg NaCl added. Since the salt effects on the two carboxylate groups of both substrates are expected to be the same, the increasing volume difference is to be attributed to the salt effect on exposing the hydroxyl group of malate to the solvent. The volume difference of 6.8 cm^3/mol with no salt added includes a volume decrease of around 5 cm^3/mol due to the exposure of the hydroxyl group to the water; by salt addition more and more constricted water is released, and a final volume difference of 11.15 cm^3/mol is attained for the two substrates.

(*d*) *The Volume Profile.* Figure 5 shows the measured volume profile at high salt concentration, including a chemical mechanism [from Cleland (1977)] that is fully consistent with

the experimental data as reviewed by Cleland (1977) and by Hill and Teipel (1971). These data were gathered from studies of the primary and secondary deuterium and tritium isotope effects, of isotopic exchange between labeled malates and either fumarate or water, of the pH variation of V and K_m and of the binding of competitive inhibitors, and of the action of fumarase on different halofumarate substrates.

There is evidence that two groups in the active site are essential for catalysis by fumarase. One is the carboxyl, which is thought to lie at the bottom of the active site, being covered by substrates. The carboxyl group holds the proton removed from malate. Imidazole from a histidyl residue is the second catalytic group. The imidazole group combines via a hydrogen bond with either the OH of the malate or the water that reacts with fumarate. Up to now one cannot tell whether the C–O or C–H bond of malate is broken first or whether the reaction is concerted, but there is some evidence that a carbonium ion intermediate is formed.

From the volume profile one can see that the binding of the substrates to the active site of the enzyme, to form the enzyme–substrate complexes EF and EM, is accompanied by a volume decrease followed by a subsequent increase. This may be explained by a conformational change enabling the transport of the substrates to the active site. On entering the enzyme, the substrates release at least some of the constricted hydration water of their carboxyl groups since the orientation of the substrates in the active site is expected to be achieved by ion pairing via one or both carboxyls; the resulting volume increase is reflected in $\Delta V^{\ddagger}_{-1}$ and $\Delta V^{\ddagger}_{3}$. There is an additional rise in volume when the hydration of fumarate or the dehydration of malate takes place ($\Delta V^{\ddagger}_{2}$ and $\Delta V^{\ddagger}_{-2}$), suggesting a voluminous intermediate $(EF = EM)^{\ddagger}$.

Only in the transition states does the volume reach a maximum or a minimum, whereas the volumes of the enzyme–substrate complexes do not differ much from the initial conditions. This, together with the striking symmetry mentioned above, indicates that the catalytic process proceeds together with a pulsation of the fumarase molecule.

The volume changes during this pulsation are small compared with the total volume of the enzyme. They are even smaller than the average volume fluctuation in proteins, which is about 0.3% of the total, as reported by Gekko and Hasegawa (1986).

Volume fluctuations originate from changing interatomic distances and cavities inside the protein. It seems that such fluctuations are aligned in enzyme catalysis, thus bringing out the volume pulsation.

Appendix

Comments upon the Use of Transition-State Theory. Kramers (1940) has shown that the velocity of chemical reactions generally depends on the viscosity of the surrounding medium. The reason is the action of Brownian motion. Only in a middle range of viscosity (not too low and not too high viscosity) is the reaction rate independent of viscosity and is then identical with that calculated via the transition-state theory (TST).

The results of Beece et al. (1980) and of Frauenfelder and Wolynes (1985) as well suggest protein reactions in water to be in the high-viscosity range. Thus eq 1 and 1a should be replaced by eq 12 and 13. Herein η is the viscosity of the

$$\left(\frac{\mathrm{d}\ln k}{\mathrm{d}p}\right)_T = -\kappa\frac{\partial \ln \eta}{\partial p} - \frac{\Delta V^{\ddagger}}{RT} \qquad (12)$$

$$k/k_0 = (\eta/\eta_0)^{-\kappa} \exp(-\Delta V^{\ddagger} p/RT) \qquad (13)$$

Table V: Slope of the ln η versus Pressure Curve of Water and Corresponding Volumes[a]

p (bar)	0–400	400–1100	1100–2400
$\partial \ln \eta/\partial p$ (bar^{-1})	-2.2×10^{-5}	0	4.74×10^{-5}
$RT(\partial \ln \eta/\partial p)$ (cm^3/mol)	−0.54	0	1.17

[a] Calculated from the data of Woolf (1975).

Table VI: Values in the Square Brackets of eq 15 for the Fumarase Reaction in Water

p (bar)	0–400	400–1100	1100–2400
$1 + (RT/\Delta V^{\ddagger}_1)(\partial \ln \eta/\partial p)$	1.013	1	0.972
$1 + (RT/U)(\partial \ln \eta/\partial p)$	0.991	1	1.020

solvent at pressure p, η_0 is the viscosity of the solvent at normal pressure, and κ is a parameter that indicates how well the reaction is shielded from the action of Brownian motion (Gavish, 1980). κ depends on the reaction step with $0 \leq \kappa \leq 1$.

The pressure dependence of the composite constant $k^{\circ} = k_1k_2/(k_{-1} + k_2)$ is obtained from eq 12 and 13 with the abbreviations $U = \Delta V^{\ddagger}_2 - \Delta V^{\ddagger}_{-1}$ and $a = k_{2,0}/k_{-1,0}$:

$$\frac{\mathrm{d}\ln k^{\circ}}{\mathrm{d}p} = -\frac{\Delta V^{\ddagger}_1}{RT} - \frac{U/RT}{1 + a(\eta/\eta_0)^{\kappa_{-1}-\kappa_2}\exp(-Up/RT)} + -\frac{\partial \ln \eta}{\partial p}\left[\kappa_1 + \frac{\kappa_2 - \kappa_{-1}}{1 + a(\eta/\eta_0)^{\kappa_{-1}-\kappa_2}\exp(-Up/RT)}\right] \qquad (14)$$

In this equation $\Delta V^{\ddagger}_i$ of the single reaction steps as well as κ_i are assumed to be pressure independent.

In water at 25 °C the value of η/η_0 hardly changes over the pressure range used in this work (Woolf, 1975). It is $0.99 \leq \eta/\eta_0 \leq 1.05$. This variation can be disregarded in comparison with that of the exponential factor. Therefore

$$(\eta/\eta_0)^{\kappa_{-1}-\kappa_2} \approx 1$$

is justified. In correspondence with this, the slope of the ln η versus p curve is small too. It is nearly constant in the below three ranges of pressure. In Table V these slopes and the corresponding volumes are given.

The integration of eq 14 yields

$$\ln\frac{k^{\circ}}{k^{\circ}_0} = -\frac{\Delta V^{\ddagger}_1}{RT}p\left[1 + \frac{\kappa_1 RT}{\Delta V^{\ddagger}_1}\frac{\partial \ln \eta}{\partial p}\right] + -\left(\ln\frac{\exp(Up/RT) + a}{1 + a}\right)\left[1 + \frac{(\kappa_2 - \kappa_{-1})RT}{U}\frac{\partial \ln \eta}{\partial p}\right] \qquad (15)$$

This equation differs from eq 9, which was used in this work to interpret the data, only by the square brackets (Table VI). Equation 15 changes into eq 9 with $(\partial \ln \eta)/\partial p = 0$ or $\kappa_1 = 0$ and $(\kappa_2 - \kappa_{-1}) = 0$. Using $\Delta V^{\ddagger}_1$ and U from Table III as a first approximation, we can calculate the values in the brackets, and assuming the most unfavorable case, $\kappa_1 = |\kappa_2 - \kappa_{-1}| = 1$.

The value is nearly equal to 1 over the whole pressure range. Therefore, it seems justified to evaluate our experimental data with eq 9 and the transition-state theory, respectively. On the other hand it seems clear that the pressure dependence of a reaction in water affords no opportunity of distinguishing between TST and Kramers theory, if the $\Delta V^{\ddagger}_i$ values are much greater than 1 cm^3/mol.

Other solvents are better suited in this respect; from the data of Collings and McLaughlin (1971) for CCl_4 at 30 °C and low pressure, e.g., one obtains

$$RT[(\partial \ln \eta)/\partial p] = 23 \text{ cm}^3/\text{mol}$$

In fact, Montgomery et al. (1979) calculated a corresponding volume contribution of 8.8 cm^3/mol for the trans–gauche isomerization of 1-butane in liquid CCl_4. This has to be compared with the TST estimation of 1.3 cm^3/mol only.

Registry No. F, 110-17-8; M, 97-67-6; fumarase, 9032-88-6.

REFERENCES

Alberty, R. A., & Pierce, W. H. (1957) *J. Am. Chem. Soc. 79*, 1526.

Alkana, R. L., Finn, D. A., Galleisky, G. G., Syapin, P. J., & Malcolm, R. D. (1985) *Science (Washington, D.C.) 229*, 772–774.

Anderson, B., & Broe, P. E. (1972) *Acta Chem. Scand. 26*, 3691–3698.

Beece, D., Eisenstein, L., Frauenfelder, H., Good, D., Marden, M. C., Reinisch, L., Reynolds, A. H., Sorenson, L. B., & Yue, K. T. (1980) *Biochemistry 19*, 5147–5157.

Bett, K. E., & Cappi, J. B. (1965) *Nature (London) 207*, 620–621.

Butz, P. (1982) Thesis, University of Heidelberg.

Butz, P. (1987) Dissertation, University of Heidelberg.

Butz, P., & Ludwig, H. (1986) *Physica (Amsterdam) 139/140B*, 875–877.

Canfield, V. A., & Macey, R. I. (1984) *Biochim. Biophys. Acta 778*, 397–384.

Cleland, W. W. (1977) *Adv. Enzymol. Relat. Areas Mol. Biol. 45*, 273–387.

Cohen, I. R. (1985) *Nature (London) 318*, 104–105.

Collings, A. F., & McLaughlin, E. (1971) *Trans. Faraday Soc. 67*, 340.

Deckmann, M., Haimovitz, R., & Shinitzky, M. (1985) *Biochim. Biophys. Acta 821*, 334–340.

Duboc, C. (1969) *Bull. Soc. Chim. Fr. 7*, 2260–2270.

Eckert, C. H. (1972) *Annu. Rev. Phys. Chem. 23*, 239–264.

Frauenfelder, H., & Wolynes, P. G. (1985) *Science (Washington, D.C.) 229*, 337–345.

Frauenfelder, H., Hartmann, H., Karplus, M., Kuntz, I. D., Jr., Kuriyan, J., Parak, F., Petsko, G., A., Ringe, D., Tilton, R. F., Jr., Connolly, M. L., & Max, N. (1987) *Biochemistry 26*, 254–261.

Gavish, B. (1980) *Phys. Rev. Lett. 44*, 1160–1163.

Gekko, K., & Hasegawa, Y. (1986) *Biochemistry 25*, 6561–6563.

Greaney, G. S., & Somero, G. N. (1979) *Biochemistry 18*, 5322–5332.

Greulich, K. O., & Ludwig, H. (1976) *Biophys. Chem. 6*, 87–94.

Heremans, K. (1978) in *High Pressure Chemistry*, Reidel, Dordrecht, Boston, and London.

Hill, R. L., & Teipel, J. W. (1971) *Enzymes (3rd Ed.) 5*, 539–568.

Kauzmann, W. (1987) *Nature (London) 325*, 763–764.

Kramers, H. A. (1940) *Physica (The Hague) 7*, 284–304.

Krebs, H., Schmid, F. X., & Jaenicke, R. (1985) *Biochemistry 24*, 3846–3852.

Laidler, K. J., & Bunting, P. S. (1973) in *The Chemical Kinetics of Enzyme Action*, pp 220–230, Clarendon, Oxford.

Le Noble, W. (1967) *Prog. Phys. Org. Chem. 5*, 207–330.

Lodge, D. (1985) *Nature (London) 314*, 386.

Low, P. S., & Somero, G. N. (1975) *Proc. Natl. Acad. Sci. U.S.A. 72*, 3305–3309.

Ludwig, H., & Greulich, K. O. (1978) *Biophys. Chem. 8*, 163–169.

Marque, J., & Eisenstein, L. (1984) *Biochemistry 23*, 5556–5563.

Massey, V. (1953) *Biochem. J. 53*, 72–79.

Mentrup, E., Butz, P., Stricker, H., & Ludwig, H. (1988) *Pharm. Ind.* (in press).

Montgomery, J. A., Jr., Chandler, D., & Berne, B. J. (1979) *J. Chem. Phys. 70*, 4056–4066.

Swezey, R. R., & Somero, G. N. (1985) *Biochemistry 24*, 852–860.

Thompson, R. B., & Lakowicz, J. R. (1984) *Biochemistry 23*, 3411–3417.

Vasetskii, S. G., Betina, M. I., & Kondrat'eva, O. T. (1985) *Dokl. Biol. Sci. (Engl. Transl.) 272*, 661.

Verjowski-Almeida, S., Kurtenbach, E., Amorim, A. F., & Weber, G. (1986) *J. Biol. Chem. 261*, 9872–9878.

Weber, G., & Drickamer, H. G. (1983) *Q. Rev. Biophys. 16*, 89–112.

Woolf, L. A. (1975) *J. Chem. Soc., Faraday Trans. 1, 71*, 784.